Noise robust spark ignition engine knock detection with redundant wavelet transform

Laurent Duval, Gilles Corde, Van Bui Tran, Pierre Leduc
Institut Français du Pétrole
1 & 4, av. de Bois-Préau
92500 Rueil-Malmaison, France
e-mail: laurent.duval@ifp.fr

1 Abstract

Spark ignition engines are subject to an abnormal combustion process called “knock”. It is associated with fast pressure increases which turn into engine vibrations causing the familiar knocking sound. Knock is a potential damage source for the piston crown or the cylinder walls. It furthermore limits engine efficiency. Fine knock detection strategies allow the engine to run at knock limit. Traditional methods involve knock detection in its frequency range using Fourier methods. Since the knock phenomenon is unsteady in time and frequency, several authors have pointed out that Fourier based analysis reaches its limits at high speed or with strong background noises. Recent research focused on time-frequency methods, such as the Wigner-Ville transforms or wavelets.

In this work, we investigate knock detection using a redundant wavelet transform which is both more robust to noise than the traditional discrete wavelet transform and still computationally efficient. The proposed scheme allows us to extract knock envelopes used for knock properties evaluations for fine control strategies. Experiments were performed on pressure and vibration signals from a 4 cylinder engine. Redundant wavelet transform knock detection is shown robust to background noises and is able to detect weak or pre-knock onsets.

2 Introduction

Spontaneous ignition of end gas in a cylinder has been recognized as the cause for spark ignition engine knock. Its fast energy release is accompanied by very fast pressure increases which turn into pressure waves. The induced resonance is transmitted to the engine structure and finally shows up as engine vibrations and the familiar knocking sound. Potential damages to the piston crown and the cylinder wall require embedded real-time spark advance control to avoid engine destruction. Finer knock detection strategies could increase engine efficiency, combustion stability, reduce transient noises and, to some extend, pollution (CO2 for instance). Traditional detection methods rely on amplitude/energy detection for one or several frequency bands, calculated from a Fourier transform or a band-pass filtered signal obtained from instrumental devices. Knock amplitude or energy is then detected using fixed or updated discriminating thresholds [1]. Though effective at low speeds, these traditional methods seem to reach their limits at high engine speed or when other noise sources interfere (background noise, injection power unit disturbances, etc.)

Several authors (e.g. [2, 3]) have pointed out that the knock signal is unsteady since chamber volume and sound speed vary through a combustion cycle. They therefore investigated “time-frequency” analysis methods such as Wigner-Ville or wavelet transforms. These methods are able to extract knock characteristics and are generally robust to background noises. For instance, wavelet transforms have generated several recent experiments [4, 5], since they combine very fast algorithms with precise ”time-frequency” features. In the present work, we propose a method based on a redundant wavelet transform that is able to extract knock properties such as envelopes, with their crank angle location and duration, and frequency range. We viewed the knock signal as a pressure oscillation around a non-knocking pressure evolution, with background noise added. The advantages of the redundant over the standard wavelet transform come from its closer approximation to a continuous wavelet transform, which yields at the same time

a better knock extraction and increased robustness against noise, at the expense of a slight computing efficiency loss. After knock extraction, we evaluate its strength relative to its location and duration in a cycle, which leads us to the analysis of its evolution from cycle to cycle. The proposed method compares favorably to Fourier and standard wavelets in terms of parameter settings and robustness to noise.

3 Introduction to knock

3.1 Requirements

The knock phenomenon is classically viewed as an abnormal combustion process. In normal combustion, a spark plug ignites a gaseous mixture of air, fuel and residual gases toward the end of the compression stroke. The mixture burns and the front flame propagates from the point of ignition to the cylinder walls and the piston crown [6].

The major theory for knock onset is auto-ignition. In this theory, unburned gases ahead from the front flame ("end gases") are compressed. The elevation of temperature and pressure may lead to a point where precombustion reactions have time to develop to a self-ignition of the unburned gases. We refer to [7] for a comparison between knock models. Auto-ignition may also start from "hot spots" in the end gases melange. The resulting impulsive pressure increase excites the cylinder cavity resonances, which are transmitted to the engine structure. It results in engine vibrations to the audible level.

Accurate detection and control strategies of knock for spark ignition (SI) engines is a valuable tool for improved engine reliability and efficiency, lower fuel consumption and a reduction of transitory noises for driver comfort [6].

Higher engine power/torque as well as fuel economy may be achieved through an increase of the engine compression ratio and the optimization of spark timing. However these two factors tend to increase knock. Other factors affect knock apparition such as fuel self-ignition resistance or cooling systems. Moreover, the risk of piston crown, cylinder wall, rings or exhaust valves damages depends on other engine operation parameters (e.g. engine speed, air-to-fuel ratio). Cylinder dependent spark advance reduction is the most commonly used method for practical dynamic knock control. The ability to accurately detect knock levels and to tune the spark advance allows engines to run close to the knock threshold, for close to optimum power and fuel consumption.

As a remark, the knocking behavior is cylinder dependent: cylinders may knock when the others do not at the same time, and knock levels may differs. It also vary from cycle to cycle, asking for cylinder dependent detection and spark advance control.

3.2 Knock definitions and properties

One of the pitfalls in knock detection arises from its definition and its "appearance". They both depends on the underlying theory and detection strategy. First, several knock definitions exists, and we will follow a generic one, from [8]:

> "Knock is an undesirable mode of combustion that originates spontaneously and sporadically in the engine, producing sharp pressure pulses associated with a vibratory movement of the charge and the characteristic sound from which the phenomenon derives its name."

Second, knock usually shows up in at least three domains: audition (knock sound), vibration and combustion (in-cylinder pressure). Though related, the transition between domains is a complex task; for instance, see e.g. [9] for the reconstruction of cylinder pressures from acceleration measurements. Moreover, knock detection, at least from audition, is partially subjective.

As a result, from these remarks, we will be interested in retrieving peaks and oscillatory waves from pressure or vibration signals. The extracted signals will be termed "knock", even though it is not the traditional knock definition. We are also interested in light oscillations which may be seen as pre-knock conditions. The main knock properties we are interested in are its variabilities:

1. in time: knock typically appears over a relatively short crank angle or time window during a cycle;
2. in amplitude: competition between the front flame and the knock generally affects the knock amplitudes;
3. in frequency: resonant frequencies depend on the dimension of the cylinder and the sound velocity. As a result, frequencies change with the piston position and the temperature, which modifies the sound velocity. Typical knock frequencies range from 5 kHz to 20 kHz;

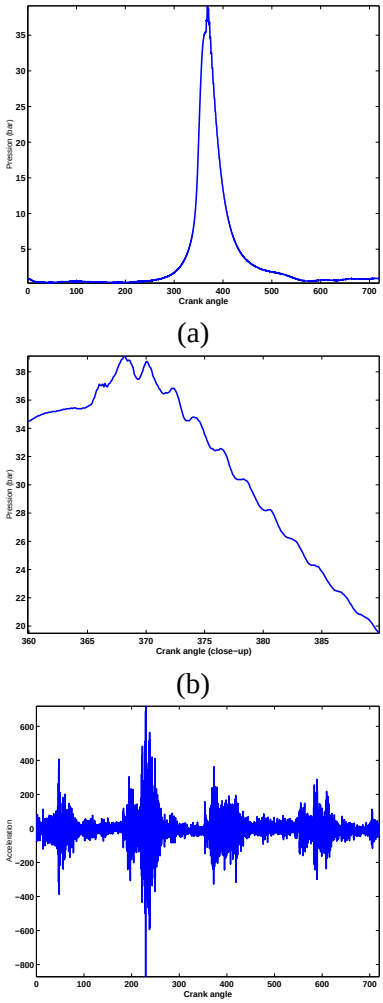

Figure 1: Knocking signal (a) in a pressure trace (b) Zoom around TDC (c) in an accelerometer trace.

4. from cycle to cycle, due to the combustion instability.

Figure 1 displays typical strong knocking pressure and vibration signals. Fig. 1–a represents the pressure trace from cylinder 2 in a 4-cylinder engine, as a function of the crank angle (CA). It exhibits a sharp peak around 370 CA (10 CA after the combustion Top Dead Center). The close-up in Fig. 1–b shows the pressure oscillations following knock onset.

Figure1–c represents the vibration with 4 combustions associated to the 4 cylinders. The relative abnormal vibration behavior of cylinder 2 shows up clearly.

3.3 Scope of the paper

In this work, we are looking for the extraction of knock signals (and parameters, subsequently) from pressure and accelerometer traces, under steady and non-steady engine operating conditions. Knock's unstationarity suggest using local signal processing techniques. We would like these methods to be robust to other engine related disturbances, as well as to background noise. The last property is crucial for accelerometer signals, as well as at high speed.

From a control perspective, we also demanded fast signal processing algorithm, to satisfy almost "real-time" requirements, and especially early knock detection (KD). Algorithm choices are detailed in the next chapter. This study is conducted in the scope of developing KD tools and KD dependent control for IFP engine test benches.

4 Introduction to knock extraction techniques

4.1 Introduction

Knock detection and estimation methods vary from simple to complex. P. V. Puzinaukas provides in [10] a thorough lists of existing methods, among which we find:

- peak pressure,
- difference between actual pressure and a smoothed pressure curve,
- pressure slope at knock onset,
- first to third order derivatives.

The most widely used methods to date are based on band-pass filtering of the pressure or the vibration signals, in the knock band-width, as in [11], with a description of hardware and software KD. The knock level is then estimated from the comparison of cumulative energy or peaks to preconditioned levels. Despite the success of these methods, most authors have recognized Fourier limitations at high speed or in noisy conditions (e.g. engine structure vibrations for acceleration signals). Moreover, even with appropriate windowing, the non-stationary of knock is not fully taken in account, as explained in the comments for Fig. 2 in Section 4.2.

Since wavelets are an effective tool for the analysis of non-stationary signals, they have been used recently in pressure analysis [12] and knock detection [13]. Their time-scale properties allow the separation of the knock signal and the other noise sources. We would like to recommend especially the reference [3].

It is a very comprehensive work on knock in general, with end-gas temperature measurements and the report of a new form of knock.

The wavelet zoom feature simplifies the detection of singular point like the knock onset. The possibility to recover multiple autoignitions in one knocking cycle, as well as potential pre-knock conditions (i.e. very weak oscillations) is also investigated.

4.2 Analysis of transient/unstationary signals: Fourier vs. wavelet

There exist a wide range of transforms for analyzing signals. We will focus here on the most widely used and emerging transforms for knock analysis, namely the Fourier and the wavelet transforms. In the following, they act on a signal $s(t)$ or its digital approximation $s(k)$.

The major difference between the continuous Fourier and wavelet transforms (resp. FT and CWT) lies in their respective analyzing kernels, respectively

- complex exponentials K_ω,
- dilations and shifts (denoted by a and b, resp.) of a template analysis function ψ called "wavelet", $K_{a,b}$.

The wavelet ψ is generally a band-pass function vanishing at $\pm\infty$.

The kernels are thus expressed as:

$$K_\omega(t) = e^{-j\omega t}, \tag{1}$$

$$K_{a,b}(t) = \frac{1}{\sqrt{a}}\psi\left(\frac{t-b}{a}\right). \tag{2}$$

The continuous Fourier and wavelet transforms of the signal $s(t)$ are given, under appropriate mathematical conditions, by :

$$F_s(w) = \int_{-\infty}^{+\infty} s(t)\, K_\omega(t)\, dt, \tag{3}$$

$$F_s(a,b) = \int_{-\infty}^{+\infty} s(t)\, K_{a,b}(t)\, dt. \tag{4}$$

We refer to [14] for detailed issues on the mathematical background. Since complex exponentials are eigenvectors of linear time-invariant operators, the FT (Fourier transform) is suitable for linear time-invariant processing. It is a invaluable tool for stationary signal analysis since each exponential spans the whole real line. As a consequence, the amplitude of each decomposition "wave" depends on the signal $s(t)$ for all values of t, mixing somewhat unrelated local information. It is hence sometimes difficult to analyze or even localize properties of transient events in a signal. It is well known that FT reaches its limits when trying to analyze a sine with steadily increasing instantaneous frequency (also known as "linear chirp"), which is not stationary. Relative feature capture skills of the FT and the CWT are represented in Fig. 2. We compose two signals from an impulse (top left) followed by a windowed sine with frequency from increasing 30 to 100 kHz (top right). The two components are arbitrarily shifted and corrupted by random noise. They produce the two signals from the second row. The third row displays their Fourier amplitude spectrum. The signals' frequency range is apparent from the spectrum but the frequency increase as well as the peak onset of the two template signals do not appear. The last row shows a frequency mapping of the CWT of the two signals. Here, the peak location (on the x-axis) shows up clearly as a bright spot at low frequencies (on the y-axis). Similarly, the frequency increase is clear from the bright stripe running from low to high frequencies. The CWT ability to detect transient time locations comes from its shift invariance: when a signal is time-shifted (or delayed), the transform will be delayed too.

For feasible real-time algorithms, a discrete equivalent of the CWT has been devised, called the discrete wavelet transform (DWT). It bears similarities with the Discrete Fourier Transform, with fast algorithms similar to that of the FFT.

4.3 Discrete and redundant wavelets

The CWT equation may be discretized following the equation:

$$\psi_{j,n}(t) = \frac{1}{\sqrt{2^j}}\psi\left(\frac{t-2^j n}{2^j}\right), \tag{5}$$

with j, n being non-negative integers. The resulting decomposition accepts a filter bank representation with an iterated building block. The building block of the DWT is a pair of digital filters, followed by decimation or downsampling operators. They are traditionally low-pass and high-pass, with finite impulse response. Since decimation cancels every second sample, the Nyquist-Shannon condition is not fulfilled anymore in the analysis stage, and spectral folding or aliasing occur. This limitation can be overcome via the choice of special filters H_i and G_i ($i \in 0, 1$),

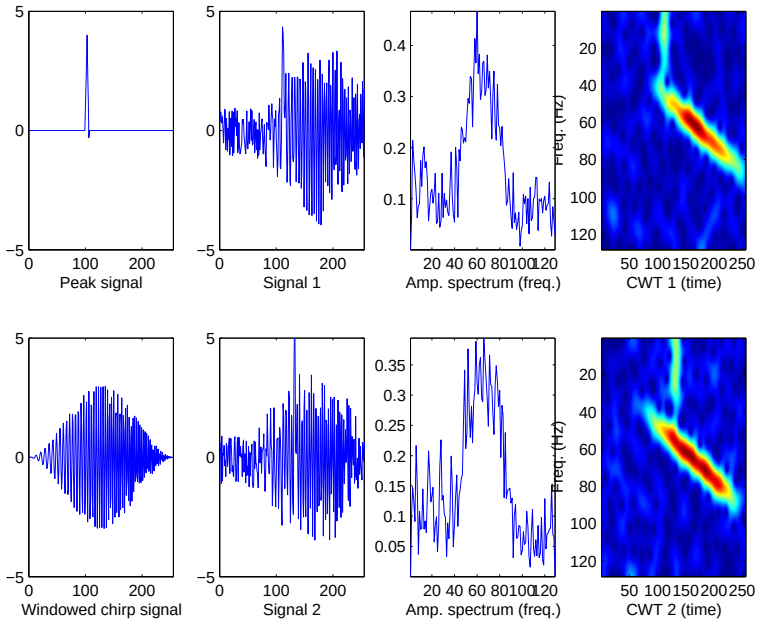

Figure 2: Peak plus chirp analysis.

as represented in Fig. 3, which suppress aliasing on the wavelet synthesis stage. We refer to [14, p. 220 sq.] for a detailed treatment on wavelets and filter banks.

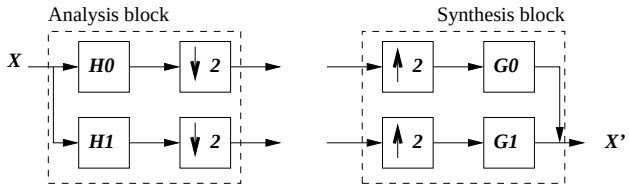

Figure 3: Classical discrete wavelet filter banks.

The classical DWT is satisfactory both in computation efficiency (there exist fast algorithms) and signal representation (N signal samples yield N wavelet coefficients, as for the FFT). But some authors have pointed out that due to downsampling, wavelet coefficients for the signals $s\,(k)$ and $s\,(k-1)$ differ. When the filter bank is iterated, more signal shifts differ because of the iteration of the analysis filter bank, depending on the dyadic decomposition level. If the wavelet decomposition spans L levels, the wavelet coefficients from the shifted signals $s\,(k)$ to $s(k-2^L-1)$ will differ. It represents a drawback in signal analysis: we would expect high transient coefficients to be simply shifted if the transient itself is shifted. Furthermore, the shift-dependence is a drawback in signal denoising [15]. The key to alleviate the dependence is to compute the wavelet transform of several signal shifts and average them out. The resulting averaged wavelet transform is less shift-dependent and more robust to noise sources.

4.4 Knock extraction from wavelet coefficients

The wavelet decomposition projects the signal onto a frame. The projecting vectors build a redundant or overcomplete wavelet representation of the signal. We retrieve coefficients from the wavelet "time/scale" plane on knock specific time/scale locations. Since the knock signal is relatively coherent, the locally concentrated associated coefficients are easily separated from the noise, and from the raw pressure signal whose frequency range is generally lower. The extracted knock is recovered from the inverse wavelet transform.

Its envelope is then computed from the low-pass rectified knock signal. The computed envelope properties are used for knocking cycle estimation.

5 Application to knock detection

5.1 Engine and experiments characteristics

The NSDI3 is a in-line 4 cylinder gasoline engine with a 1150 cm3 total displacement (see Table 1). It is a direct injected, stratified charge engine that has been designed and realized by IFP.

Type	In line, 4 cyl.
Displacement	1150 cc
Bore $\times$ stroke	69 $\times$ 76.9
Compression ratio	11.0 : 1

Table 1: Main features of IFP-NSDI3 engine.

The engine is fitted with a 10mm, water cooled, AVL pressure sensor and a conventionnal accelerometer (serial produced for the automotive industry and used on the vehicle for knock control). The engine was tested under several engine operating conditions, with steady or unsteady spark advance. The figures displayed in the following sections were taken from experiments at 4000 RPM (rounds-per-minutes).

5.2 Fourier/wavelet noise sensitivity

Figure 4 shows the relative noise sensitivity of a band-pass knock filtering technique and the proposed redundant wavelet based knock envelope extraction. The top left image displays a strong knocking pressure trace, on a window between 350 and 390 CA (crank angle). The top right image shows the knock signal filtered by a traditional band-pass Butterworth filter (dotted line) and the wavelet envelope (solid line). Both knock extraction methods are reliable, since the pressure signal is relatively clean from other noise sources and the knock level is relatively high. The first peak is easily detected by a threshold above the amplitude of the knocking signal between 350 and 360 CA. The slight difference comes from the estimated peak amplitude at the beginning of the knock onset. Fourier filtering tends to smooth peaks, while wavelets are able to accurately extract such singularities. As a result, the peak amplitude might be slightly underestimated with classical filtering techniques.

On the bottom images, the same detections are simply performed on the same pressure trace with random noise added. As we can see from the bottom right image, threshold based detection is more involved with Fourier technique, since the signal level before knock is only 2 times lower than the maximum knock peak. The wavelet estimation, though not as faithful as without noise, still exhibits a before/after peak ratio greater than 3.

Similar remarks can be made regarding the detection of low pre-knock levels, since the knock signal to ambient noise ratio becomes comparable to that of the noisy knock extraction.

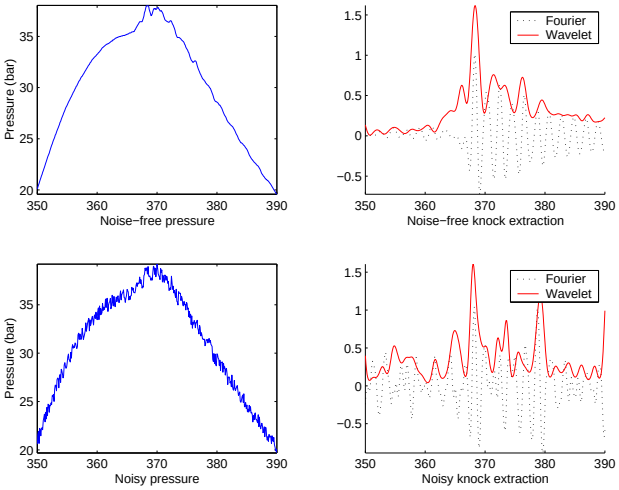

Figure 4: Comparison between Fourier based and wavelet envelope knock extraction.

5.3 Knock signal extraction

The experiments in this section focus on knock extraction with several spark advance conditions. The engine is run under constant speed and charge. From left to right and top to bottom in Fig. 7, 120 consecutive cycles were recorded respectively with:

1. constant optimum spark advance (no knock),
2. constant knocking spark advance (knock),
3. variation of the spark advance (from no knock to knock),
4. variation of the spark advance (from knock to no knock).

For figures clarity, only every 4th cycle is displayed, with cycle indexes ranging from 1 to 30. Signals are also displayed in a CA window from 350 to 390. The first remark concerns cycle to cycle variability. Under optimal spark advance (Fig. 7 top left), pressure peaks vary in excess of 30 %, between 22 and 30 bars. A similar remark holds under knocking conditions (Fig. 7 top right): the typical knock bumps appear sporadically, with varying levels. The second remark concerns operating conditions: with a variation of spark advance settings (Fig. 7 bottom), knock increase or decrease is relatively hard to control precisely, because of the somewhat stochastic knock onset behavior, and the short duration of 120 cycles (about 3.6 s at 4000 RPM).

Figure 8 displays the knock envelopes related to the pressure signals from Figure 7. The top left image at optimum spark advance exhibits low amplitude envelopes (under 0.4 bar), but some signals (e.g.

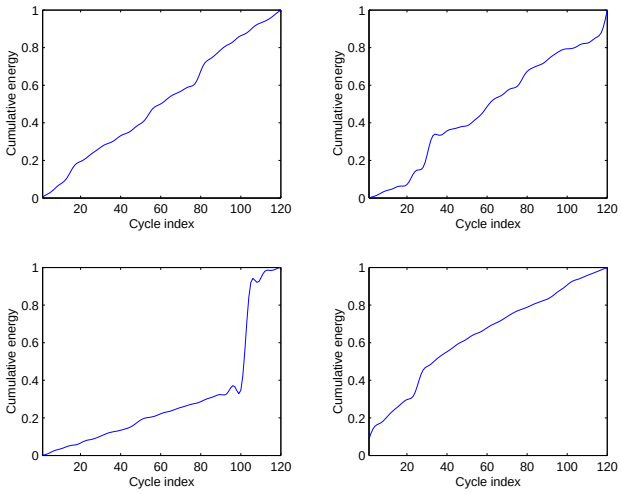

Figure 5: Normalized cumulative energies for the 4 engine operating conditions.

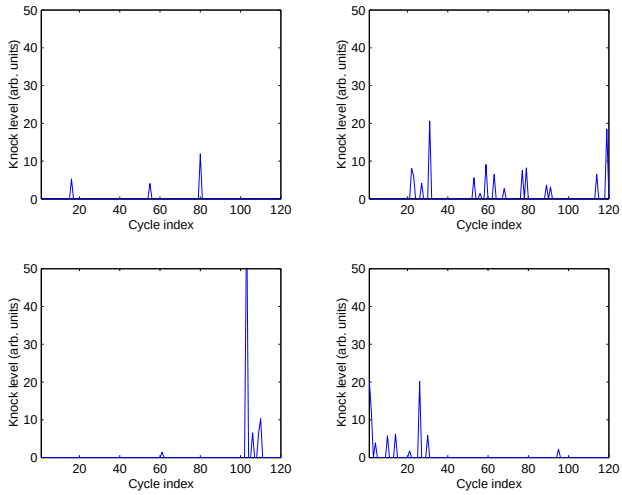

Figure 6: Tentative knock detection.

around the 13th cycle index) seem to behave like pre-knock, with a peak and evolving instantaneous frequencies. The top right image shows clearer knock signals, which appear stochastically above 0.6 bar. The bottom images display envelopes that generally increase or decrease in amplitude and area respectively.

We also note that the knock envelopes location moves during the consecutive cycles. Knock location could be useful for predicting the destructive effect of the knock, depending on the piston crown location in the cylinder. Finally, multi-modal knock envelopes seem to indicate potential multiple knock onsets in one cycle.

5.4 Knock properties extraction

Figure 5 represents the normalized cumulative energies for the 4 engine operating conditions. The energies are filtered to account for consecutive cycles. The two top images, relative to stationary behavior (without and with knock), show a (relatively) linear behavior, indicating that the knock properties do not change drastically. The two bottom images exhibit respectively a concave and convex trends, showing the increase or decrease of knock strength.

5.5 Tentative knock detection

The final question concerns the knock detection by itself: when is there knock, when not? As quoted in Section 3.2 from [10], knock detection levels depend at least on knock definition. We are not able in this work to give a general enough knock definition that would satisfy all needs. Finer knock detection may require further experiments to estimate simultaneously the reduction of knock side effects (engine damage, noise reduction, CO2 exhausts) as a function of the spark timing control strategies, and the balance thereof.

We are investigating a family of knock detection methods. There are based on:

- knock envelope extraction,
- determination of the non-knocking baseline (before and after the potential knock onset range),
- computation of the norm of above baseline knocking signals (usually a L_p norm).

Figure 6 represents knock detection results for the above operating conditions. Using the proposed redundant wavelet knock extraction and a simple L_2 norm, the following remarks are made:

- from the top left image, knock seems to exist at low levels, but is very rare, and thus harmless,
- in knocking cycles (top right image), detected knocks are stronger and more frequent, but still oddly distributed,
- detected knock distribution increases or decreases accordingly to the spark advance.

The apparent stochastic knock behavior still represents a problem and require further experiments, at this point of the study. Several other knock properties could be evaluated as well (CA location, sparsity, etc.)

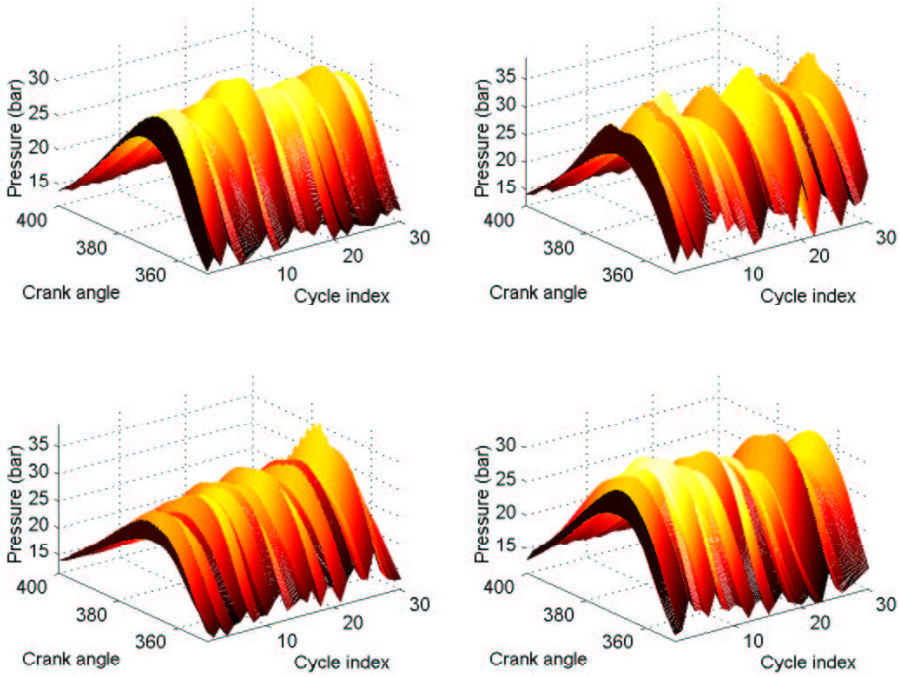

Figure 7: Four sets of cycles with several spark advance conditions.

6 Conclusions and perspectives

We propose a method for spark ignition engine knock detection, based on a redundant wavelet transform. The chosen transform yields precise peak determination and oscillatory waves extraction from pressure and vibration signals. The proposed scheme compares favorably to Fourier based methods in terms of noise robustness and knock properties extraction. It is suggested that knock-like signals with weaker amplitudes exist when knock is not detected using traditional frequency based methods. We are currently implementing the validated method in the scope of engine test benches knock detection tools and associated spark timing control.

Further experiments will involve the selection of an appropriate set of knock properties for optimal real-time spark advance control. The correlation between pressure and vibration trace is also investigated to avoid the use of engine intrusive sensors.

7 Acknowledgments

This study was financially supported by the Institut Français du Pétrole (IFP). The first author would like to thank especially Jean-Pierre Dumas and Dominique Soleri (IFP) for useful talks on the knock phenomenon, Christophe Dufresnes (IFP), for test bench data acquisition, Franz Regul for initial knock tests methods and Klaas Burgdorf (Volvo, Sweden), for providing us with his “overcomplete” PhD thesis.

References

[1] W. R. Leppard. Individual-cylinder knock occurence and intensity in multicylinder engines. In *SAE Technical Paper 820074*, 1982.

[2] B. Samimy, G. Rizzoni, and K. Leisenring. Improved knock detection by advanced signal processing. In *SAE International Congress and Exposition*, 1995. SAE Paper 950845.

[3] Klaas Burgdorf. *Engine Knock: Characteristics and Mechanisms*. PhD thesis, Chalmers University of Technology, Department of Thermo and Fluid Dynamics, Gothenburg, Sweden, Dec. 1999.

[4] K. Burgdorf and I. Denbratt. Comparison of cylinder pressure based knock detection methods. *SAE Transactions*, 1997. SAE Paper 972932.

[5] Zhong Zhang and Eiji Tomota. A new diagnostic method of knocking in spark-ignition engine using the wavelet transform. In *International spring fuels and Lubricants meeting and exposition*, Paris, June 2000. SAE Paper 2000–01–1801.

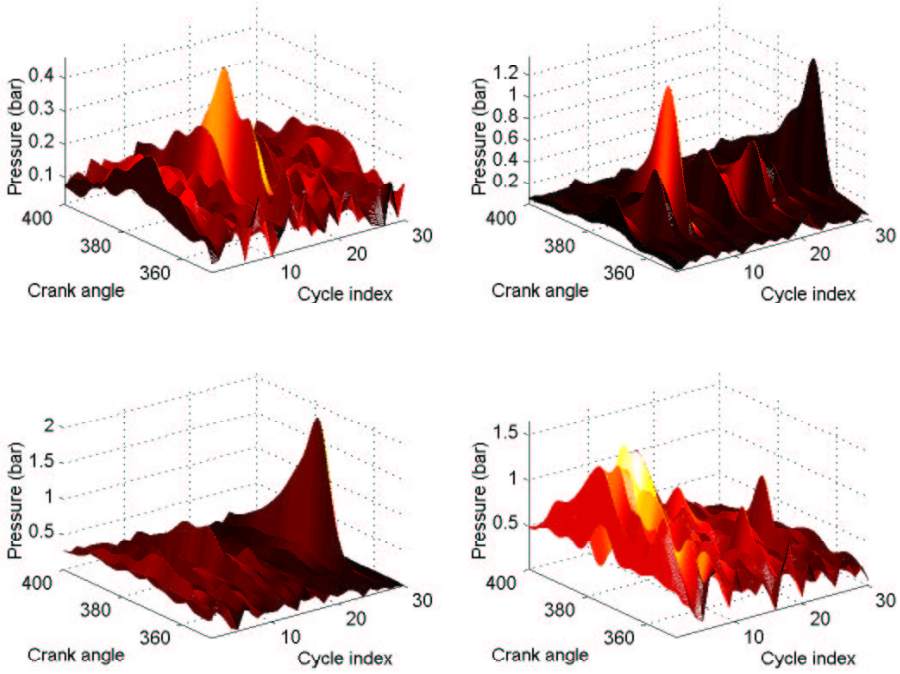

Figure 8: Corresponding four knock's envelopes.

[6] John Wagner, John Keane, Robert Koseluk, and William Whitlock. Engine knock detection: products, tools, and emerging research. In *SAE International Congress and Exposition*, Detroit, Michigan, USA, 1998. Society of Automotive Engineers. SAE Paper 980522.

[7] Ph. Pinchon. Analysis of available knock models including a comparison with experiments on CFR and automotive engines. In *EC - Combustion research. Contractors meeting on European Community, Brussels*, pages 115–123, Apr. 19-20 1988.

[8] A. K. Oppenheim. The knock syndrome — its cures and its victims. *SAE Transactions*, 93(5):874–883, 1984. SAE Paper 841339.

[9] G. Zurita, A. Ågren, R. B. Randall, and Y. Gao. Reconstruction of cylinder pressure time trace on a six-cylinder from acceleration measurements. In *Proceedings ISMA 23, Noise and Vibration Enginnering*, Sep. 1998.

[10] Paulius V. Puzinauskas. Examination of methods used to characterize engine knock. In *SAE Technical Paper Series*, 1992. SAE paper 920808.

[11] Thomas G. Horner. *Engine knock detection using spectral analysis techniques with a TMS320 DSP*. Digital Signal Processor Systems — Semiconductor Group, Aug. 1995.

[12] C. Mobley. Wavelet analysis of non-intrusive pressure transducer traces. In *SAE International Congress and Exposition*. Society of Automotive Engineers, 2000. SAE Paper 2000-01-0931.

[13] H. Kikuchi, M. Nakashizuka, H. Watanabe, and A.N. Willson, Jr. Fast nonorthogonal wavelet transforms and reconstructions for detonation detection. In *Int. Symp. on Circ. and Syst.*, pages 503–506, 1993.

[14] Stéphane Mallat. *A wavelet tour of signal processing*. Academic Press, 1998.

[15] A. Siebert. A linear shift invariant multiscale transform. In *Int. Conf. on Image Processing*, 1998.